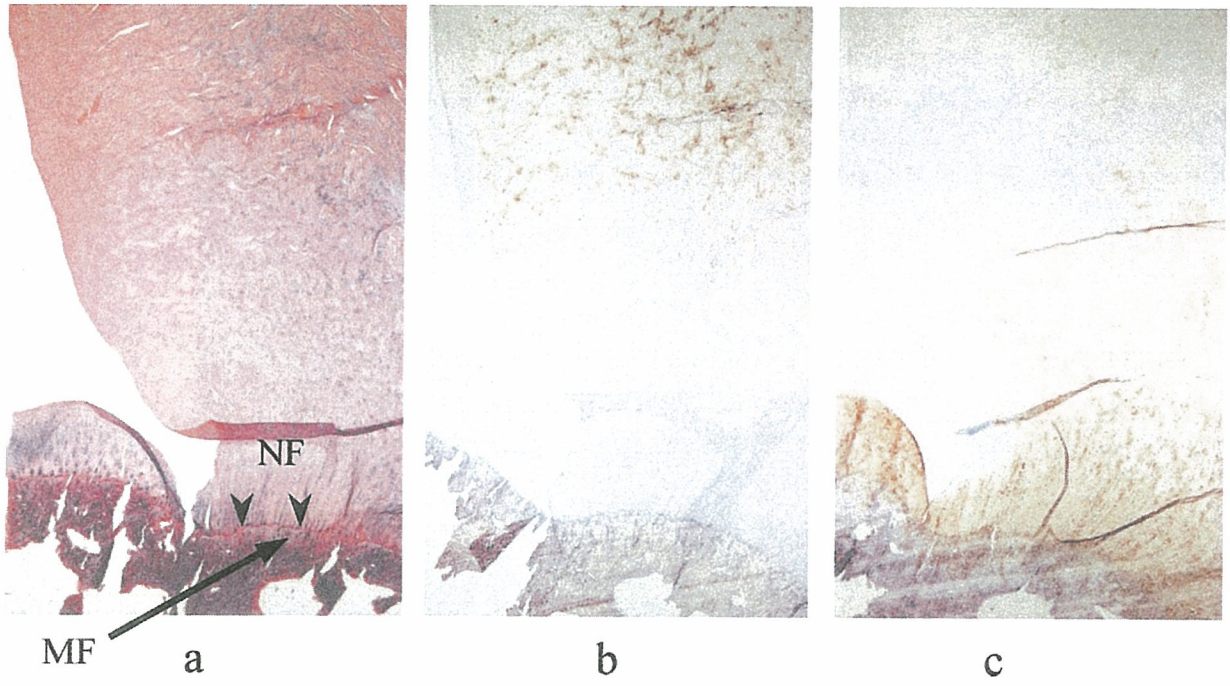

Figure 3 Higher magnification of the supraspinatus tendon insertion (Original magnification = ×4.00). (**a**) Hematoxylin-eosin; (**b**) type I collagen; (**c**) type II collagen. There is a distinct line (tidemark) between the non-mineralized fibrocartilage (NF) and the mineralized fibrocartilage (MF), which is a calcifying front (*arrowhead*). Both the non-mineralized and the mineralized fibrocartilage are positively stained with type II collagen.

supraspinatus tendon. Unfortunately, the insertion site was not included in their study. Thus, this is the first study measuring the material properties of each zone in the supraspinatus tendon insertion.

The advantages of applying SAM for such heterogeneous soft tissues are 3-fold. First, the material properties of each type of tissue can be measured non-destructively. Second, the preparation of specimens is simple, because only formalin-fixed paraffin sections are required. Such specimens can be used not only for routine histologic staining but also for immunohistochemical staining. Third, the distribution of the acoustic properties can be displayed in 2 dimensions. These 3 advantages enable a better understanding of the tissue material properties as well as comparisons with the histologic or the immunohistochemical characteristics.

The tissue sound speed measured with SAM was directly proportional to the square value of its Young's modulus (Equation 2). In other words, the sound speed (c) could be used as a parameter of the tissue material properties, especially the elasticity.[18] SAM also provides another acoustic parameter, the attenuation constant. Although the attenuation constant is not a pure physical parameter, it has a close relationship with the absorption of the ultrasound in the material.[18] The absorption by the tissue is known to be affected by its molecular weight and viscosity.[19] Moreover, the attenuation constant has a strong correlation with the sound speed. In the measurement of atherosclerotic human aorta with SAM, both the attenuation constant and the sound speed were lower in fatty plaque than in normal intima. On the other hand, both of them showed higher values in calcified plaques or fibrosis.[17]

In the current study, the acoustic properties corresponded well to the mineralization and the predominant collagen type. Accordingly, both the sound speed and the attenuation constant were the lowest in the non-mineralized fibrocartilage (type II collagen) among the 4 zones of the insertion site. Histologically, the direction of the tendon fibers was markedly changed at the non-mineralized fibrocartilage.[5] It was reported that the amount of non-mineralized fibrocartilage was greatest at sites where the change of the fiber angle was the most significant.[1,2] Moreover, recent finite element analysis revealed that the non-mineralized fibrocartilage is exposed not only to tensile force but also to compressive force.[27] Based on these findings, it was assumed that the non-mineralized fibrocartilage dissipates stress away from the insertion site.[9] We speculate that the variations in the Young's modulus at the insertion site may represent adaptations in response to biomechanical stress.

There were several limitations in the current study. First, the anatomy of the rabbit shoulder is different

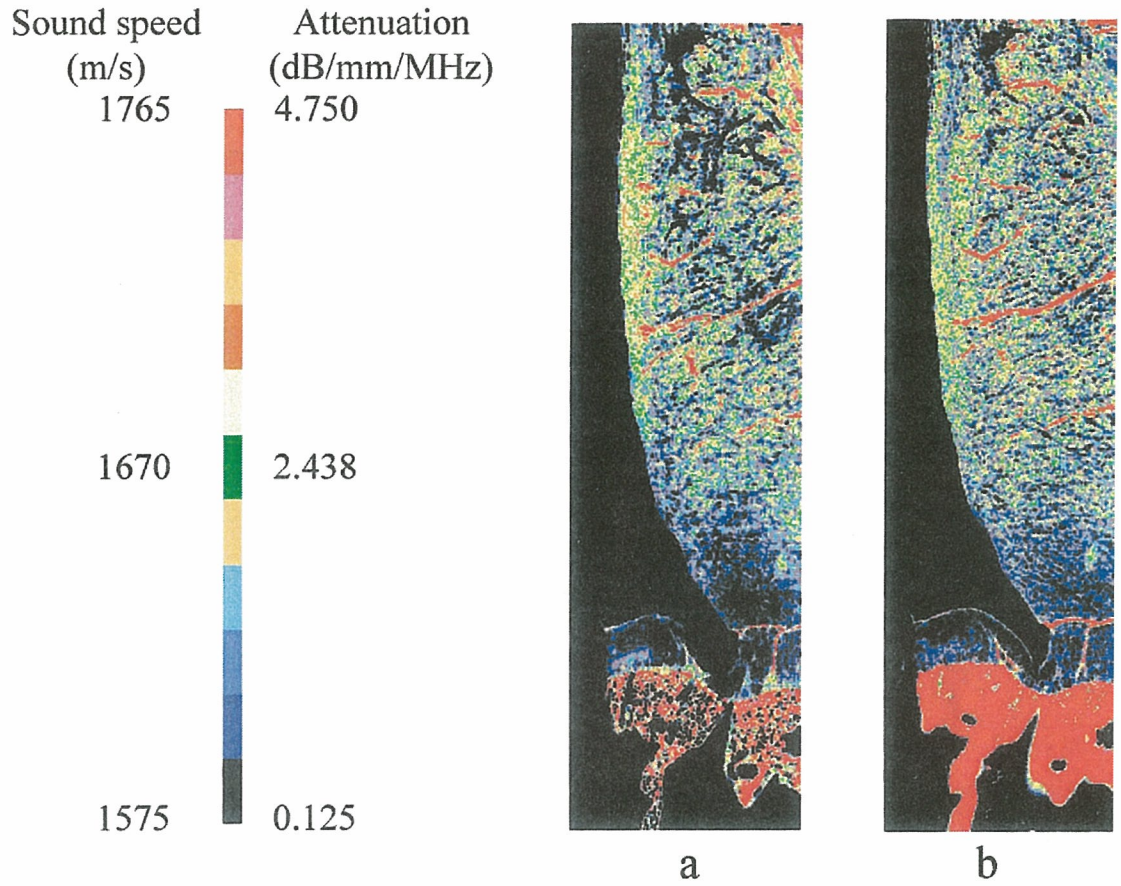

Figure 4 Two-dimensional distribution of the acoustic properties. (**a**) Sound speed; (**b**) attenuation constant. The 2-dimensional distribution of the sound speed and that of the attenuation constant show almost identical patterns. In the tendon proper and the non-mineralized fibrocartilage, these values gradually decrease with the change in the predominant collagen from type I to type II.

from that of humans.[24] Although the histologic structure of the rabbit supraspinatus tendon insertion is similar to that of humans,[8] its function differs. Second, the preparation of the tissue for SAM might alter the acoustic properties of the specimens, for example, formalin fixation, dehydration, paraffin embedding, etc. However, it has been already confirmed that such methods do not change significantly the tissue acoustic properties.[23] Thus, we believed that the relative relationships of the acoustic properties in the specimen would be preserved in the SAM measurement. Third, the Poisson's ratio and the density of the tissue should be measured at the microscopic level to determine the exact Young's modulus of the tissue.

The rabbit specimens measured in the current study did not exhibit any degenerative changes. In the clinical setting, partial thickness tears are frequently seen at the articular surface of the supraspinatus tendon insertion.[4] It has been thought that intrinsic degeneration is the primary pathogenetic factor in such partial thickness tears.[20,26] However, it is still unknown why degeneration occurs at this site. In the current study, we confirmed that the material properties of the supraspinatus tendon varied with the histologic characteristics. The elasticity of the tissue dramatically changed at the site of the tidemark, a calcifying front. Further investigations, including human specimens, would be needed to clarify the effects of the tissue material properties on the pathogenesis of degeneration and tendon tearing at the insertion site.

CONCLUSIONS

The acoustic properties of the supraspinatus tendon at the insertion were measured using SAM. Both the sound speed and the attenuation constant were the lowest in the non-mineralized fibrocartilage among the 4 zones of the insertion. These variations in the material properties at the insertion site could be interpreted as representing an adaptation to various types of biomechanical stress.

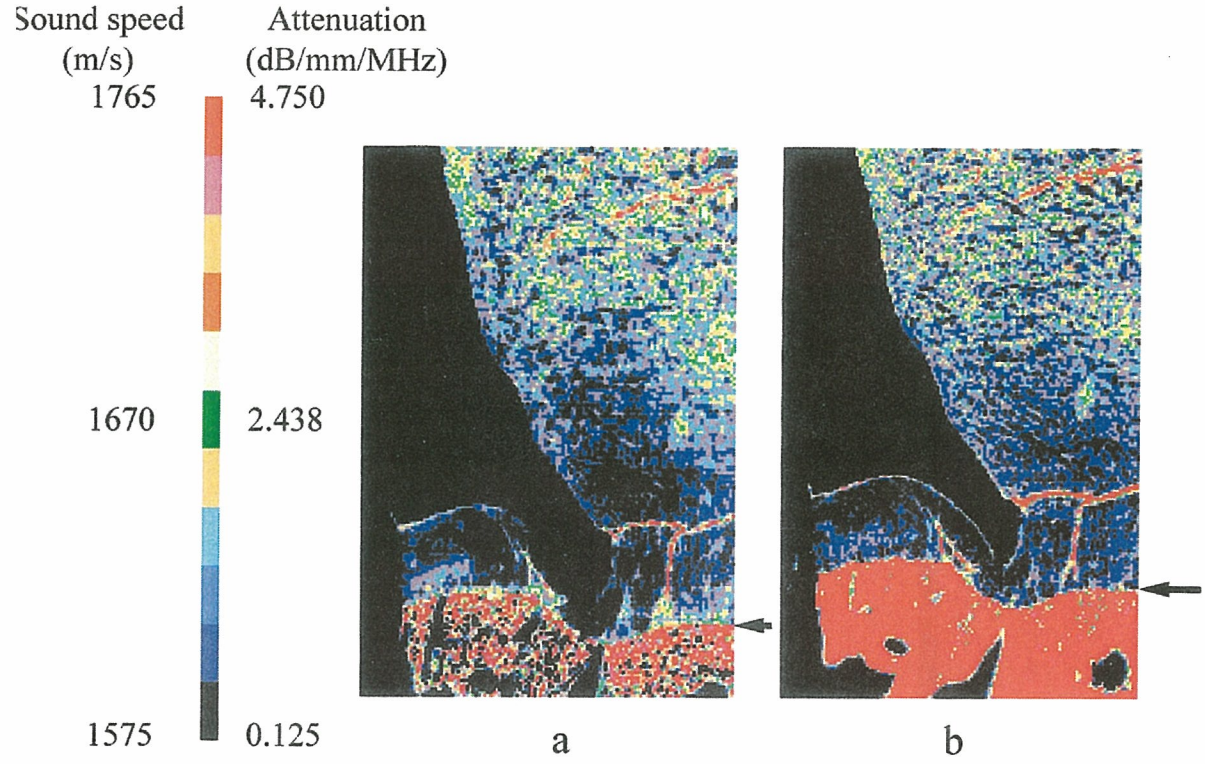

Figure 5 Acoustic properties at the supraspinatus tendon insertion. (**a**) Sound speed; (**b**) attenuation constant. The acoustic properties change dramatically at the tidemark (*arrow*). Both the sound speed and the attenuation constant indicate higher values in the mineralized fibrocartilage than in the non-mineralized fibrocartilage.

Table I The attenuation constant and the sound speed of each tissue at the supraspinatus tendon insertion

	Attenuation constant (dB/mm/MHz)	Sound speed (m/sec)
Tendon proper	2.225–3.065	1661–1695
Non-mineralized fibrocartilage	0.125–0.965	1575–1609
Mineralized fibrocartilage	4.330–4.750	1731–1765
Bone	4.330–4.750	1731–1765

REFERENCES

1. Benjamin M, Evans EJ, Rao RD, Findlay JA, Pemberton DJ. Quantitative differences in the histology of the attachment zones of the meniscal horns in the knee joint of man. J Anat 1991;177:127-34.
2. Benjamin M, Newell RLM, Evans EJ, Ralphs JR, Pemberton DJ. The structure of the insertions of the tendons of biceps brachii, triceps and brachialis in elderly dissecting room cadavers. J Anat 1992; 180:327-32.
3. Benjamin M, Ralphs JR. Fibrocartilage in tendons and ligament—an adaptation to compressive load. J Anat 1998;193: 481-94.
4. Codman EA. The shoulder. Boston, MA: Thomas Todd Company; 1934. p. 65–107.
5. Cooper RR, Misol S. Tendon and ligament insertion. A light and electron microscopic study. J Bone Joint Surg Am 1970;52A: 1-20.
6. Hasegawa K, Turner CH, Recker RR, Wu E, Burr DB. Elastic properties of osteoporotic bone measured by scanning acoustic microscopy. Bone 1995;16:85-90.
7. Itoi E, Berglund LJ, Grabowski JJ, et al. Tensile properties of the supraspinatus tendon. J Orthop Res 1995;13:578-84.
8. Kumagai J, Sarkar K, Uhthoff HK, Okawara Y, Ooshima A. Immunohistochemical distribution of Type I, II and III collagens in the rabbit supraspinatus tendon insertion. J Anat 1994;185:279-84.
9. Kumai T, Takakura Y, Rufai A, Miltz S, Benjamin M. The functional anatomy of the human anterior talofibular ligament in relation to ankle sprains. J Anat 2002;200:457-65.
10. Lee S-B, Nakajima T, Luo Z-P, Zobitz ME, Chang Y-W, An K-N. The bursal and articular sides of the supraspinatus tendon have a different compressive stiffness. Clin Biomechanics 2000;15: 241-7.
11. Lemons RA, Quate CF. A scanning acoustic microscope. Proc IEEE Ultrasound Symp 1973:18-20.
12. Matyas JR, Anton MG, Shrive NG, Frank CB. Stress governs tissue phenotype at the femoral insertion of the rabbit insertion of the rabbit MCL. J Biomechanics 1995;28:147-57.
13. Nakajima T, Rokuuma N, Hamada K, Tomatsu T, Fukuda H. Histologic and biomechanical characteristics of the supraspinatus tendon: reference to rotator cuff tearing. J Shoulder Elbow Surg 1994;3:79-87.
14. Okawai H, Tanaka M, Chubachi N, Kushibiki J. Non-contact simultaneous measurement of thickness and acoustic properties of a biological tissue using focused wave in a scanning acoustic microscope. Jpn J Appl Physiol 1987;26:52-4.

15. Saijo Y, Tanaka M, Okawai H, Dunn F. The ultrasonic properties of gastric cancer tissues obtained with a scanning acoustic microscope system. Ultrasound Med Biol 1991;17:709-14.
16. Saijo Y, Tanaka M, Okawai H, Sasaki H, Nitta S-I, Dunn F. Ultrasonic tissue characterization of infarcted myocardium by scanning acoustic microscopy. Ultrasound Med Biol 1997;23:77-85.
17. Saijo Y, Sasaki H, Okawai H, Nitta S-I, Tanaka M. Acoustic properties of atherosclerosis of human aorta obtained with high-frequency ultrasound. Ultrasound Med Biol 1998;24:1061-4.
18. Saijo Y, Chubachi N. Microscopy. Ultrasound Med Biol 2000; 26(Suppl 1):S30-2.
19. Saijo Y, Jorgensen C S, Falk E. Ultrasonic tissue characterization of collagen in lipid-rich plaques in apoE-deficient mice. Atherosclerosis 2001;158:289-95.
20. Sano H, Ishii H, Backman DS, Brunet JA, Trudel G, Uhthoff HK. Structural disorders at the supraspinatus tendon insertion—their relation to tensile strength. J Bone Joint Surg Br 1998;80B:720-5.
21. Sano H, Saijo Y, Kokubun S. Material properties of the supraspinatus tendon at its insertion—a measurement with the scanning acoustic microscopy. J Musculoskeletal Res 2004;8:29-34.
22. Sano H, Wakabayashi I, Itoi E. Stress distribution in the supraspinatus tendon with partial-thickness tears: an analysis using two-dimensional finite element model. J Shoulder Elbow Surg 2006; 15:100-5.
23. Sasaki H, Saijo Y, Tanaka M, et al. Influence of tissue preparation on the high-frequency acoustic properties of normal kidney tissue. Ultrasound Med Biol 1996;22:1261-5.
24. Soslowsky LJ, Carpenter JE, DeBano CM, Banerji I, Moalli MR. Development and use of an animal model for investigations on rotator cuff disease. J Shoulder Elbow Surg 1996;5:383-92.
25. Turner CH, Rho J, Takano Y, Tsui TY, Pharr GM. The elastic properties of trabecular and cortical bone tissues are similar: results from two microscopic measurement techniques. J Biomechanics 1999;32:437-41.
26. Uhthoff HK, Sano, H. Pathology of failure of the rotator cuff tendon. Orthop Clin North Am 1997;28:31-41
27. Wakabayashi I, Itoi E, Sano H, et al. Mechanical environment of the supraspinatus tendon: a two-dimensional finite element model analysis. J Shoulder Elbow Surg 2003;12:612-7.

Upsala J Med Sci 111 (3): 303–313, 2006

Increased Elasticity of Capsule After Immobilization in a Rat Knee Experimental Model Assessed by Scanning Acoustic Microscopy

Yoshihiro Hagiwara[1]*, Yoshifumi Saijo[2], Eiichi Chimoto1, Hirotoshi Akita[3], Yasuyuki Sasano[3], Fujio Matsumoto[1], Shoichi Kokubun[1]

[1]*Department of Orthopaedic Surgery, Tohoku University Graduate School of Medicine, Sendai, 980-8574, Japan*
[2]*Department of Medical Engineering and Cardiology, Institute of Development, Aging and Cancer, Tohoku University, Sendai 980-8575, Japan*
[3]*Division of Craniofacial Development and Regeneration, Tohoku University Graduate School of Dentistry, Sendai, Japan*

Abstract

Objectives: The mechanical property of immobilized joints is not well understood. The present study was designed to investigate the tissue elasticity of the anterior and posterior synovial membrane (SM) in a rat immobilized knee model using scanning acoustic microscopy (SAM). Moreover, the structural characteristics of the SM after immobilization were examined by transmission electron microscopy (TEM).

Methods: Thirty rats had their knee joints immobilized with a plate and metal screws. The rats were fixed at 1, 2, 4, 8 and 16 weeks after surgery and the knee joints were sectioned sagittally for SAM. Selected specimens were processed for TEM. A new concept SAM using a single pulsed wave instead of continuous waves was applied to measure the sound speed of the anterior and posterior SM, comparing it with the corresponding light microscopic images.

Results: The sound speed of the posterior SM increased significantly in the 8- and 16-week experimental group compared with that in the control group. The sound speed of the anterior SM showed no statistical difference between the experimental and the control groups at any period of immobilization. The posterior SM of the experimental group was different from that of the control group in the ultrastructural characteristics of extracellular matrices.

Conclusions: Our data suggest that the increased elasticity and structural changes of the posterior SM are one of the main causes of limited extension after a long period of immobilization in flexion using SAM, which is a powerful tool for evaluating the elasticity of targeted tissues.

Introduction

Joint contracture is defined as a decrease in both active and passive ranges of motion (ROM) after immobilization. The decreased ROM limits the activity of daily living in various aspects. Immobilization, which is a major cause of joint contracture, is beneficial for decreasing pain caused by trauma and preventing the joint from damage in the acute phase of arthritis such as pyogenic and rheumatoid arthritis [1–3]. Even by extensive rehabilitation or surgical treatment, however, it is difficult to regain the full ROM in an established joint contracture after a long period of immobilization [4,5].

Received 17 February 2006
Accepted 21 March 2006

The components of joint contracture after immobilization are classified into arthrogenic and myogenic ones. The arthrogenic components are lesions of bone, ligaments, capsule and synovial membrane (SM), while the myogenic components are lesions of muscle, tendon and fascia [6,7]. Some investigators have attributed contracture to myogenic causes (8), while others attributed it to arthrogenic causes [4,7,9–13]. It is difficult to evaluate such contradictory reports because different animal species and methods were used in their immobilization experiments. Among the arthrogenic components, the stiffness of the capsule and SM through synovial atrophy, retraction, fibrosis, and adhesion may contribute to the limited ROM [1,7,8,10,14–17]. Though increased elasticity of the capsule or SM has been suggested to be a cause of joint contracture [18], it is not known how the elasticity and the structural characteristics of extracellular matrices are affected by immobilization.

A scanning acoustic microscopy (SAM) using continuous waves characterize biological tissues by determining the elastic parameters based on the sound speed [19]. Recent studies on infarcted myocardium [20], atherosclerosis of aorta [21] and carotid arterial plaques [22] have shown that the acoustic properties reflect the collagen types. In the present study, we applied a new concept SAM using single pulsed wave, which can make total time for calculation significantly shorter, to examine the elasticity of the anterior and posterior SM (synovial intima and subintima) in the course of knee joint immobilization in a rat experimental model.

Material and Methods

Animals. The protocol for this experiment was approved by the Animal Research Committee of Tohoku University. Adult male Sprague-Dawley rats weighing from 380 to 400 g were used. Their knee joints were immobilized at 145° in flexion by rigid internal but extra-articular fixation for various periods (1, 2, 4, 8 and 16 weeks) according to a previously described method (1). The left and right hind legs were immobilized alternately to avoid potential systematic side differences. The surgery was performed under anesthesia with sodium pentobarbital (50 mg/kg) administered intraperitoneally. A rigid plastic plate (POM-N, Senko Med. Co., Japan) implanted subcutaneously joined the proximal femur and the distal tibia away from the knee joint and was solidly held in place with one metal screw (Stainless Steel, Morris, J. I., Co., USA) at each end. The knee joint capsule and the joint itself were untouched. Postoperative analgesia with buprenorphine (0.05 mg/kg) was injected subcutaneously. Sham operated animals had holes drilled in the femur and tibia and screws inserted but none of them were plated. The animals were allowed unlimited activity and free access to water and food. The immobilized animals and the sham operated animals made up the experimental groups and the control groups, respectively. Thirty rats (1, 2, 4, 8 and 16 weeks) were prepared. Each group was composed of 6 experimental and 5 control animals.

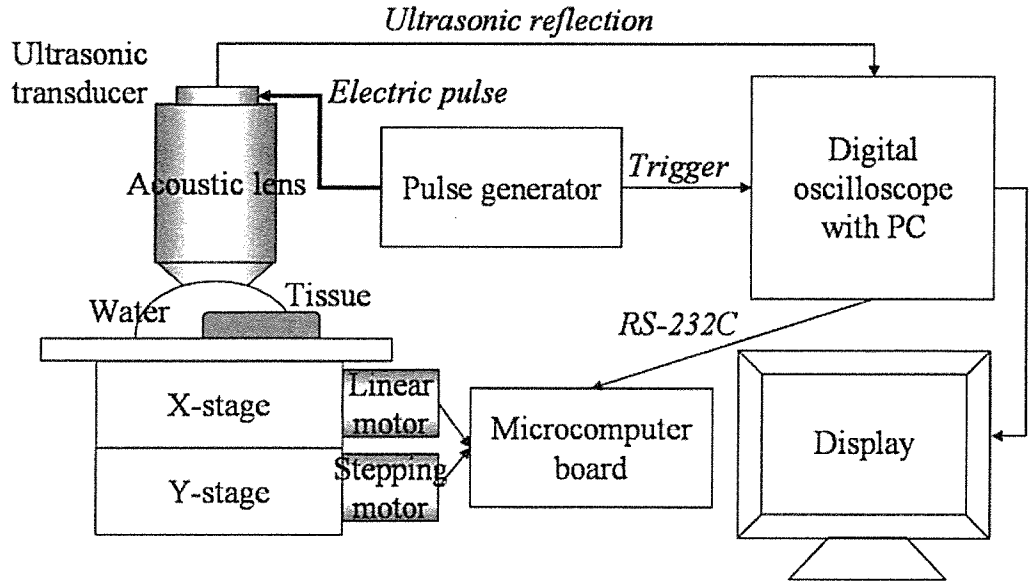

Figure 1. Schematic illustration of a new concept scanning acoustic microscopy (SAM). A new concept SAM can make total time for calculation significantly shorter than a conventional SAM by using a single pulsed wave instead of continuous waves.

Tissue preparation. The rats were anesthetized and fixed with 4% paraformaldehyde in 0.1M phosphate-buffer, pH7.4 by perfusion through the aorta. The knee joints were resected and kept in the same fixative overnight at 4C°. The fixed specimens were decalcified in 10% EDTA in 0.01M phosphate-buffer, pH7.4 for 1–2 months at 4C°. After dehydration through a graded series of ethanol solutions, the specimens were embedded in paraffin. The embedded tissue was cut into 5-μm thick sagittal sections from the medial to the lateral side of the joint. Standardized serial sections of the medial midcondylar region of the knee were made.

The serial sections were prepared for hematoxylin-eosin stain to observe the histological appearance of SM after immobilization.

Scanning acoustic microscopy. Our SAM consists of five parts: 1) ultrasonic transducer, 2) pulse generator, 3) digital oscilloscope with PC, 4) microcomputer board and 5) display unit (Figure 1). A single pulsed ultrasound with 5 ns pulse width was emitted and received by the same transducer above the specimen. The aperture diameter of the transducer was 1.2 mm and the focal length was 1.5 mm. The central frequency was 80 MHz and the pulse repetition rate was 10 kHz. Considering the focal distance and the sectional area of the transducer, the diameter of the focal spot was estimated as 20 μm at 80 MHz. Distilled water was used as the coupling medium between the transducer and the specimen. The reflections from the tissue surface and from interface between the tissue and the glass were received by the transducer and were introduced into a digital oscilloscope (Tektronics TDS 5052,

USA). The frequency range was 300 MHz and the sampling rate was 2.5 GS/s. Four pulse responses at the same point were averaged in the oscilloscope in order to reduce random noise.

The transducer was mounted on an X–Y stage with a microcomputer board that was driven by the computer installed in the digital oscilloscope through an RS-232C. The X-scan was driven by a linear servo-motor and the Y-scan was driven by a stepping motor. Finally, two-dimensional distributions of the ultrasonic intensity, sound speed and thickness of the 2.4 by 2.4 mm specimen area were visualized with 300 by 300 pixels. The total scanning time was 121 sec.

Signal analysis. The reflected waveform comprises two reflections at the surface and the interface between the tissue and the glass. The thickness and sound speed were calculated by Fourier-transforming the waveform [19].

Image analysis. Normal light microscopic images corresponding to the stored acoustic images were captured (DMLB 100 HC light microscope, LEICA Wetzlar, Germany). A region of analysis by SAM was set in the anterior and posterior SM each in each section (Figure 2). In the region, the sound speed of SM, excluding meniscus, bone and cartilage, was calculated with a gray scale SAM images using commercially available image analysis software (PhotoShop 6.0, Adobe Systems Inc., San Jose, CA) (Figure 4). SAM images with a gradation color scale were also produced for clear visualization of the sound speed. The optical and acoustic images were compared to ensure morphological congruence in the analysis.

Transmission electron microscopy. The posterior SM of 8-week experimental and control groups were fixed with a mixture of 0.04% glutaraldehyde and 4.0% paraformaldehyde in 0.1M phosphate-buffered saline, pH 7.4, at 4C° into the intra-articular space for rapid fixation. The skin around the knee was excised and the posterior SM was immersed with the same fixative for 1h at 4C°. After washed thoroughly with Dulbecco's PBS to remove the fixative, the tissue was cut with a razor blade into pieces and post-fixed with 2% buffered osmium tetroxide. The tissues were stained en bloc in aqueous uranyl acetate solution, dehydrated through a graded series of ethanol solutions and embedded in EPON 812 resin (TAAB Laboratory Equipment Ltd). Ultrathin resin sections of the specimens were mounted on copper, counterstained with uranyl acetate and Reynold's lead citrate solution, then observed with a Hitachi H-9000 electron microscope [23].

Statistics. All data were expressed as the mean ± SD. The statistical significance of difference in the results was evaluated by unpaired analysis of variance, and P values were calculated by Tukey's method. A P value less than 0.05 was considered statistically significant.

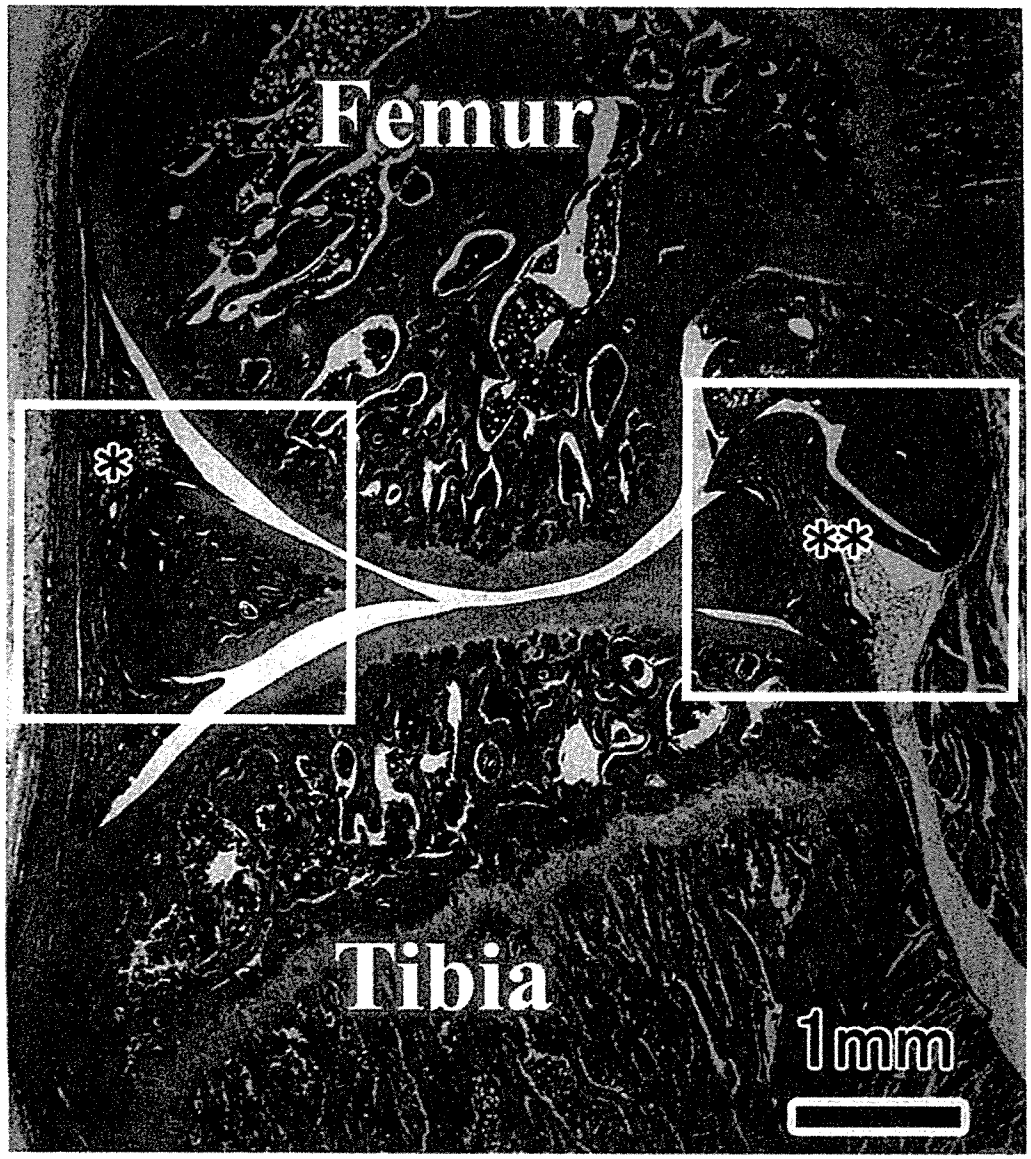

Figure 2. Microphotograph of a sagittal section in the medial midcondylar region of a rat knee. Squares indicate regions of analysis by scanning acoustic microscopy in the anterior(＊) and posterior(＊＊) synovial membrane. (Original magnification × 10, hematoxylin-eosin stain)

Results

SAM examination. The gradation color images of the posterior SM in the experimental group differed from those in the control group (Figure 3). The posterior SM was composed of low sound speed areas (black to blue) in 2-week immobilization (Figure 3A). The low sound speed area decreased and high sound speed areas (yellow to red) gradually increased in the posterior SM of the experimental group

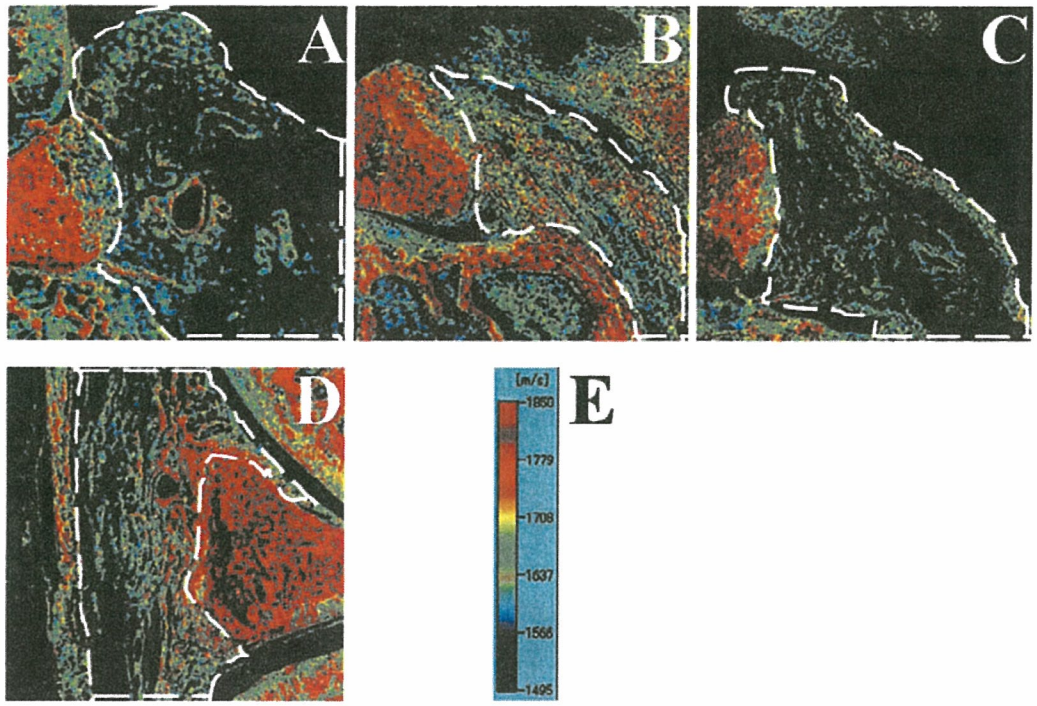

Figure 3. Gradation color images of scanning acoustic microscopy in the posterior and the anterior synovial membrane (SM). **A**, 2-week immobilization group (posterior). **B**, 16-week immobilization group (posterior). **C**, a representative of the control groups (posterior, 16-week). **D**, a representative of the control group (anterior, 16-week). **E**, gradation color table. Most low sound speed areas (black to blue) were replaced by high sound speed area (yellow to red) over time in the posterior experimental group. The posterior SM in the control groups remained entirely black to blue throughout the duration. The anterior SM was similar in the experimental and control group irrespective of the immobilization periods. Regions enclosed with a dotted line indicate the SM for calculation.

with time (Figure 3B). The posterior SM remained same in all the control groups (Figure 3C).

The anterior SM was similar in all the experimental and control groups irrespective of immobilization periods (Figure 3D).

The sound speed of the posterior SM is shown in Figure 4. There was no statistical difference between the experimental and the control groups in 1-, 2- or 4-week immobilization (1w: 1560 m/s±18.7 m/s vs. 1543 m/s±16.3 m/s; $p = 0.152$, 2w: 1552 m/s±26.0m/s vs. 1535 m/s±8.17 m/s; $p = 0.207$, 4w: 1551 m/s±4.01 m/s vs. 1553 m/s±13.3 m/s; $p = 0.698$). In 8- and 16-week immobilization, however, the sound speed in the experimental group was significantly higher than that in the control group (8w: 1546 m/s±18.7 m/s vs. 1646 m/s±11.8 m/s; $p = 6.69 \times 10^{-6}$, 16w: 1568 m/s±26.5 m/s vs. 1677 m/s±32.8 m/s; $p = 1.06 \times 10^{-4}$) (Figure 4A). There was no statistical difference in the anterior SM in all the experimental and the control groups at any period of immobilization (1w: 1563 m/s±22.7 m/s vs. 1556 m/s±13.8 m/s; $p = 0.545$, 2w: 1562 m/s±12.4 m/s vs. 1565 m/s±11.4 m/s; $p = 0.74$, 4w: 1559 m/s±10.1 m/s vs. 1554 m/s±30.4 m/s; $p = 0.745$, 8w: 1550m/

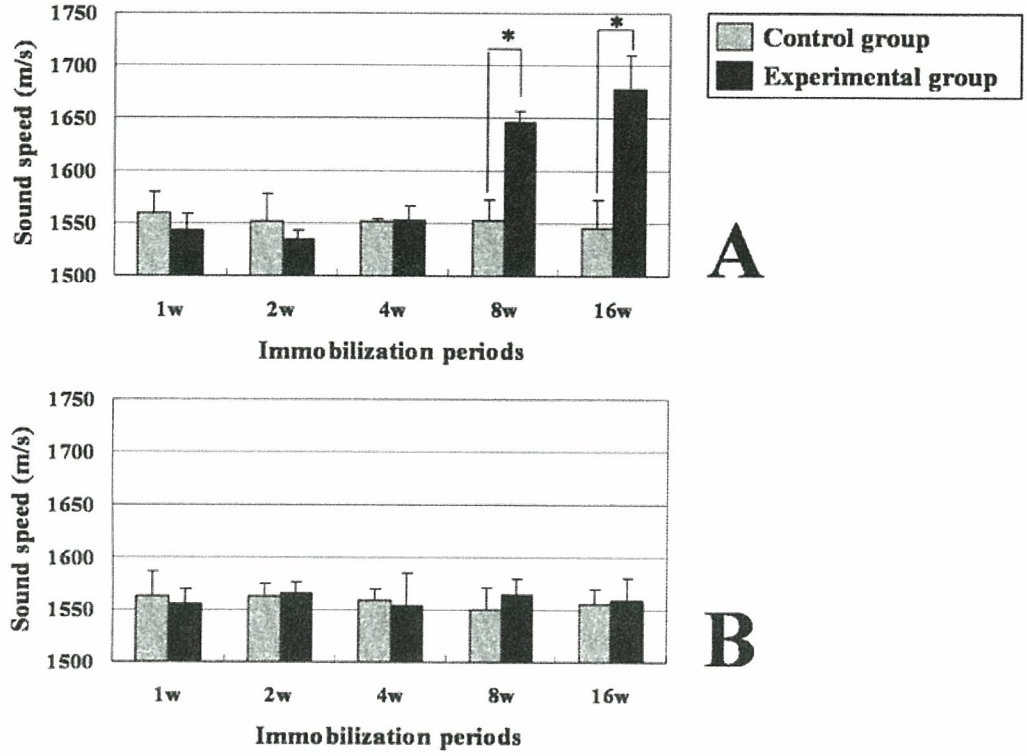

Figure 4. Sound speed changes of the posterior and the anterior synovial membrane (SM). **A**, the posterior SM. **B**, the anterior SM. In the posterior SM, significant difference of sound speed is seen in 8- and 16-week immobilization. There was no statistical difference at any period of immobilization in the anterior SM. solid bars = experimental groups, shaded bars = control groups. Values are the mean ± SD. * = $P < 0.005$ versus control, by Tukey's method.

s ± 20.5 m/s vs. 1564 m/s ± 15.3 m/s; p = 0.263, 16w: 1556 m/s ± 14.1 m/s vs. 1558 m/s ± 22.6 m/s; p = 0.846) (Figure 4B).

TEM examination. In the experimental group, the space among collagen bundles and cells were occupied with the high density matrix, which fills the interspace of collagen microfibrils within the collagen bundle. In contrast, the high density matrix surrounding cells, collagen bundles and fibrils were scarce in the control group (Figure 5).

Discussion

The arthrogenic component has been considered as an important factor of joint contracture after immobilization (1,7,8,10,14–18). In a study using a rabbit knee contracture model, the mechanical characteristics were quantified by a torque-angular displacement diagram [18]. Knees in 9-week immobilization in flexion showed a significantly larger torque in extension in the experimental group than in the control

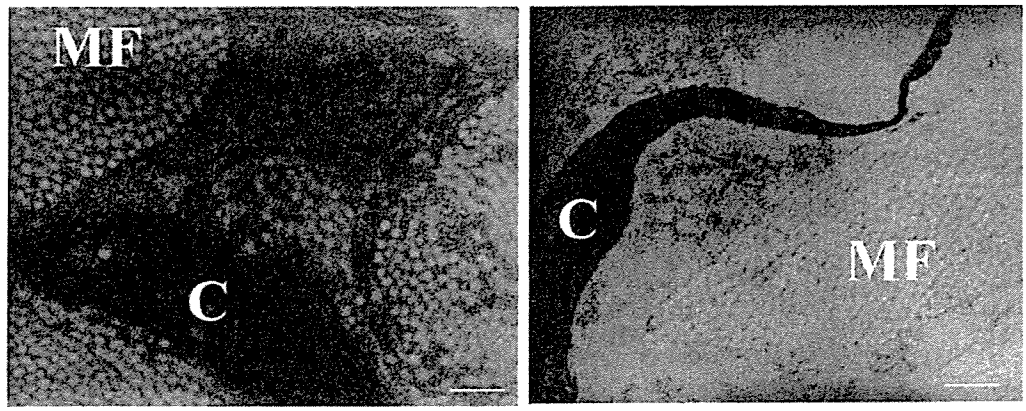

Figure 5. Structural characteristics of the posterior synovial membrane (SM). **A**, 8-week experimental group. **B**, 8-week control group. Compared with the control group, the space among collagen bundles and cells were occupied with the high density matrix, which fills the interspace of collagen microfibrils within the collagen bundle in the experimental group. ***C***, cell; ***MF***, microfibrils. (Original magnification × 360,000, scale bar = 0.5 μm).

group even after total extra-articular myotomies. In the same rat model as ours in the present study but immobilized up to 32 weeks, ROM in extension still remained restricted even after total extra-articular myotomies [7]. In canine glenohumeral joint immobilized up to 16 weeks, the intra-articular pressure rose higher by injection of Hypaque contrast medium and the filling volume was smaller compared with the control group at a rupture of the capsule [24]. These studies suggest that among the arthogenic components, the capsule and SM may mostly contribute to production of joint contracture.

Connective tissue proliferation in the SM and its adhesion to articular cartilage in the intra-articular space has been considered as pathological features of contracture after immobilization [25–29]. But conflicting studies with it have been reported. No intra-articular connective tissue proliferation occurred after immobilization [1,30–32]. No contact between the connective tissue and articular cartilage was observed [32]. In the same rat model as ours in the present study but immobilized up to 32 weeks, the decrease in the synovial intima length was observed after 4-week immobilization [1]. This study concluded that mutual adhesions of synovial villi rather than the connective tissue proliferation were the major pathophysiological changes leading to contracture. Further, the decrease of the synovial intima length was reported to be greater in the posterior SM than in the anterior SM in the same model as ours in the present study [1]. It may be explained as earlier mutual adhesion of synovial villi in the posterior SM under less tension with the knee immobilized in flexion.

Connective tissue response after immobilization is important to understand the mechanism of the increased elasticity of the posterior SM. Some suggestions con-

cern changes in the biochemical composition of periarticular fibrous connective tissue (e.g. patellar tendon, ligament and joint capsule) after immobilization. The notable change was a reduction of water and glycosaminoglycans without decreased collagen mass [9,18,32,33]. These changes were expected to alter plasticity and pliability of connective tissue matrices and to reduce lubrication efficiency [32].

In the same rat model as ours in the present study but immobilized up to 32 weeks, the posterior subintimal area of the experimental groups was smaller than that of the control groups through all the immobilization periods [1]. This result may reflect the decreased water and glycosaminoglycans of the SM. Our TEM observation showed that the space among collagen bundles and microfibrils was occupied with dense matrices in the experimental group, which may reflect the synovial atrophy due to decreased water content but not increased extracellular matrices. Further, adhesions of collagen bundles may limit lubrication and increase elasticity.

Previous studies analyzed the elasticity of the joint as a whole including ligament, capsule and SM with or without muscles [7,15,18,24]. But it was impossible to evaluate the elasticity of the individual arthrogenic components, especially of capsule and SM in those studies. The present study is the first that measured the elasticity of SM in situ by SAM in rat immobilized knees and revealed the increased elasticity of the posterior SM, subsequent to the inhibition of extension to cause the joint contracture. One reason why the elasticity is different between the anterior and the posterior SM of 8- and 16-week experimental group may be that compared with the posterior SM immobilized rigidly, the anterior SM keeps motion to a larger extent after immobilization with patella while being active. The present study suggested that the increased elasticity and structural changes of the posterior SM are one of the main causes of limited extension after immobilized in flexion.

Acknowledgements

The authors would like to acknowledge their valued input and efforts of Mr. Katsuyoshi Shoji, Mrs. Michiko Fukuyama and Miss Haruka Sasaki and thank Dr. Hans K Uhtoff and Dr. Guy Trudel for their technical advice of making the animal model.

References

1. Trudel G, Seki M, Uhthoff HK (2000) Synovial adhesions are more important than pannus proliferation in the pathogenesis of knee joint contracture after immobilization: an experimental investigation in the rat. J Rheumatol 27:351–357.
2. Patridge REH, Duthie JJR (1963) Controlled trial of the effect of complete immobilization of the joints in rheumatoid arthritis. Ann Rheum Dis 22:91–99.
3. Gault SJ, Spyker JM (1969) Beneficial effect of immobilization of joints in rheumatoid and related arthritis: A splint study using sequential analysis. Arthritis Rheum 12:34–44.
4. Peacock EE (1966) Some biochemical and biophysical aspects of joint stiffness: Role of collagen synthesis as opposed to altered molecular bonding. Ann Surg 164:1–12.

5. Damron TA, Greenwald TA, Breed A (1994) Chronological outcome of surgical tendoachilles lengthing and natural history of gastro-soleus contracture in cerebral palsy. Clin Orthop 301:249–255.
6. Trudel G. (1997) Differentiating the myogenic and arthrogenic components of joint contractures. An experimental study on the rat knee joint. Int J Rehabil Res 20:397–404.
7. Trudel G, Uhtoff HK (2000). Contractures secondary to immobility: is the restriction articular or muscular? An experimental longitudinal study in the rat knee. Arch Phys Med Rehabil 81:6–13.
8. Evans BE, Eggers GWN, Butler JK, Blumel J (1960) Experimental immobilization and remobilization of rat knee joints. J Bone Joint Surg 42A:737–758.
9. Amiel D, Akeson WH, Harwood FL, Mechanic GL (1980) The effect of immobilization on the types of collagen synthesized in periarticular connective tissue. Connect Tissue Res 8:27–32.
10. Enneking WF, Horowits M (1972) The intra-articular effects of immobilization on the human knee. J Bone Joint Surg 54A:973–985.
11. Hall MC (1963) Cartilage changes after experimental immobilization of the knee joint of the young rat. J Bone Joint Surg 45A:35–44.
12. Wilson PD (1944) Capsulectomy for the relief of flexion contractures of the elbow following fracture. J Bone Joint Surg 26A:71–86.
13. Wagner LC (1948) Fixed extension of the knee due to capsular contraction. NY State J Med 48:194–198.
14. Trudel G, Desaulniers N, Uhthoff HK, Laneuville O (2001) Different levels of COX-1 and COX-2 enzymes in synoviocytes and chondrocytes during joint contracture formation. J Rheumatol 28:2066–2074.
15. Trudel G, Uhthoff HK, Brown M (1999) Extent and direction of joint motion limitation after prolonged immobility: an experimental study in the rat. Arch Phys Med Rehabil 80:1542–1547.
16. Finsterbush A, Friedman B (1973) Early changes in immobilized rabbit knee joints: a light and electron microscopic study. Clin Orthop 92:305–319.
17. Roy S (1970) Ultrastructure of articular cartilage in experimental immobilization. Ann Rheum Dis 29:634–642.
18. Woo SL, Matthews JV, Akeson WH, Amiel D, Convery FR (1975) Connective tissue response to immobility: Correlative study of biomechanical measurements of normal and immobilized rabbit knees. Arthritis Rheum 18:257–264.
19. Hozumi N, Yamashita R, Lee CK, Nagao M , Kobayashi K, Saijo Y, Tanaka M, Tanaka N, Ohtsuki S (2004) Time-frequency analysis driven ultrasonic microscopy for biological tissue characterization. Ultrasonics 42:717–722.
20. Saijo Y, Tanaka M, Okawai H, Sasaki H, Nitta S, Dunn F (1997) Ultrasonic tissue characterization of infracted myocardium by scanning acoustic microscopy. Ultrasoud Med Biol 23:77–85.
21. Saijo Y, Sasaki H, Okawai H, Nitta S, Tanaka M (1998) Acoustic properties of atherosclerosis of human aorta obtained with high-frequency ultrasound. Ultrasound Med Biol 24:1061–1064.
22. Saijo Y, Jorgensen S, Mondek P, Sefranek V, Paaske W (2002) Acoustic inhomogeneity of carotid arterial plaques determined by GHz frequency range microscopy. Ultrasound Med Biol 28:933–937.
23. Sasano Y, Ohtani E, Narita K, Kagayama M, Murata M, Saito T, Shigenobu K, Takita H, Mizuno M, Kuboki Y (1993) BMPs Induce Direct Bone Formation in Ectopic Sites Independent of the Endochondral Ossification In Vivo. Anat Rec 236:373–380.
24. Shollmeier G, Sarkar K, Fukuhara K, Uhtoff HK (1996) Structural and functional changes in the canine shoulder after cessation of immobilization. Clin Orthop 323:310–315.
25. Schollmeier G, Uhtoff HK, Sarkar K, Furuhara K (1994) Effects of immobilization on the capsule of the canine glenohumeral joint. Clin Orthop 304:37–42.
26. Evans BE, Eggers GWN, Butler JK, Blumel J (1960) Experimental immobilization and remobilization of rat knee joints. J Bone Joint Surg 42A:737–758.
27. Enneking WF, Horowits M (1972) The Intra-articular effects of immobilization on the human knee. J Bone Joint Surg 54A:973–985.
28. Thaxter TH, Mann RA, Anderson CE (1965) Degeneration of immobilized knee joints in rats. J Bone Joint Surg 47A:567–585.
29. Hall MC (1963) Cartilage changes after experimental immobilization of the knee joint of the young rat. J Bone Joint Surg 45A:35–44.

30. Matsumoto F, Trudel G, Uhtoff HK (2002) High collagen type I and low collagen type III levels in knee joint contracture: an immunohistochemical study with histological correlate. Acta Orthop Scand 73:335–343.
31. Sood SC (1971) A study of the effects of experimental immobilization on rabbit articular cartilage. J Anat 108:497–507.
32. Akeson WH, Woo SL, Amiel D, Coutts RD, Daniel D (1973) The connective tissue response to immobility: biochemical changes in periarticular connective tissue of the immobilized rabbit knee. Clin Orthop 93:356–362.
33. Akeson WH, Amiel D and La Violette D (1968) The connective tissue response to immobility: An accelerated aging response? Exp Gerotol 3:289–301.

Corresponding author:
Yoshihiro Hagiwara
1-1 Seiryo-machi, Aoba-ku,
Sendai 980-8574, Japan
e-mail: hagi@mail.tains.tohoku.ac.jp
Tel: +81-22-717-7245
Fax: +81-22-717-7248